J|A|C|S
COMMUNICATIONS

Published on Web 06/20/2003

On-Chip Integration of Enzyme and Immunoassays: Simultaneous Measurements of Insulin and Glucose

Joseph Wang,* Alfredo Ibáñez, and Madhu Prakash Chatrathi

Department of Chemistry and Biochemistry, New Mexico State University, Las Cruces, New Mexico 88003

Received May 11, 2003; E-mail: joewang@nmsu.edu

Microfabricated fluidic devices are of considerable recent interest.[1,2] Such technology offers great promise for developing powerful and versatile miniaturized analyzers compatible with future requirements.[3] Because of these advantages, microchip platforms have proven themselves as attractive vehicles for conducting enzymatic[4−6] and immunological[7−9] assays. The resulting biochips combine the analytical power of microfluidic devices with the inherent selectivity of biocatalytic and immunological reactions. Simultaneous enzymatic and immunological biochip measurements of the corresponding substrates and antigens have not been demonstrated, despite the fact that such bioassays have long been the backbone of clinical diagnostics.

This Communication reports on a novel biochip concept integrating immunochemical and enzymatic assays within the same microchannel to allow simultaneous measurements of glucose and insulin. The simultaneous monitoring of insulin and glucose, and hence of the insulin/glucose ratio, is of great relevance for the management of diabetes, the detection of pancreatic islet cell malfunction, the definition of hypoglycemia, and the diagnosis of insulinoma.[10−12]

As illustrated in Figure 1, the realization of such dual-bioassay single-channel microchip protocol involves the judicious coupling of multiple enzymatic and immuno reactions through integration of electrophoretic separations with relevant pre- and postcolumn reaction steps. Such a biochip operation is thus comprised of precolumn reactions of the enzyme-labeled antibody (anti-human insulin) with its antigen (insulin) and the reaction of the glucose-dehydrogenase (GDH) enzyme with its glucose substrate in the presence of its NAD^+ cofactor; these are followed by electrophoretic separation of the free antibody, antibody−antigen complex, and the NADH product of the glucose enzymatic reaction, and a postcolumn reaction of the alkaline-phosphatase (ALP) enzyme tag with its *p*-nitrophenyl phosphate (*p*-NPP) substrate. Both the NADH and the *p*-nitrophenol (*p*-NP) products are monitored at the downstream amperometric detector.

Such an ability to conduct simultaneous on-chip enzyme and immunoassays is demonstrated in Figure 2. Electropherograms were first recorded to identify the individual peaks of the new glucose/insulin biochip protocol and to demonstrate that the new biochip responds independently to glucose and insulin. An injection of the ALP-labeled anti-insulin alone, coupled to the postcolumn addition of the *p*-NPP substrate, resulted in a well-defined "free-antibody" peak at around 160 s (A,a). Similarly, injecting glucose along with GDH and NAD^+ led to a defined NADH peak at around 236 s (B,b). Two resolved peaks, with similar (160 and 236 s) migration times, are observed upon conducting the glucose assay in the presence of the enzyme-labeled antibody (C,a,b). Repeating the experiment in the presence of an excess (1 μM) of insulin resulted in a well-defined peak (around 394 s) of the labeled immunocomplex and the disappearance of the "free-antibody" peak (D). The latter indicates the completeness of the immunological reaction

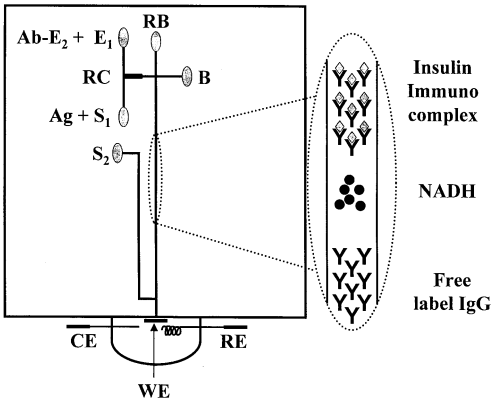

Figure 1. Schematic of the biochip used for simultaneous immunological and enzymatic assays. (RB) Running buffer, (Ab-E_2) alkaline phosphatase-labeled anti-insulin, (E_1) GDH enzyme, (Ag) insulin, (S_1) glucose, (RC) reaction chamber, (S_2) *p*-NPP, (B) buffer, (WE) working electrode, (CE) counter electrode, and (RE) reference electrode. See text for dimensions and details.

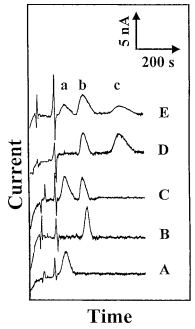

Figure 2. (A) Electropherograms for the ALP-labeled antibody (1.28×10^{-4} g mL^{-1}) in connection to a postcolumn addition of the *p*-NPP substrate (at 20 mM). (B) Response for 1 mM glucose in the presence of GDH and NAD^+ (20 U mL^{-1} and 20 mM, respectively). (C) Same as B but in the presence of ALP-labeled antibody (1.28×10^{-4} g mL^{-1}) and *p*-NP (20 mM). (D) Same as C but in the presence of 1 μM insulin. (E) Same as D but in the presence of 0.3 nM insulin. Separation and postcolumn voltages, 1500 V; injection, 5 s at 1000 V; detection potential, +1.2 V (vs Ag/AgCl wire).

because of the large excess of the antigen. Finally, the same experiment was performed in the presence of a substantially lower (0.3 nM) insulin concentration to yield three defined and resolved peaks (at similar migration times) for the free-labeled antibody, the NADH (glucose-enzymatic) product, and the labeled immunocomplex (E,a−c). Using the free-antigen peak for quantitation (instead of the complex signal) allows significantly (40%) shorter assay times. Coexisting electroactive compounds, for example, ascorbic and uric acids, are expected to migrate between the glucose and labeled immunocomplex peaks and are not expected to interfere.

Relevant experimental parameters affecting the dual immuno/enzyme response were assessed and optimized. For example,

10.1021/ja036067e CCC: $25.00

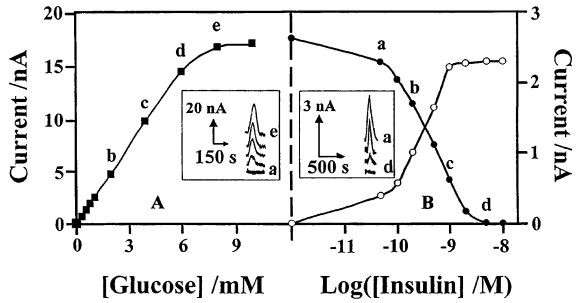

Figure 3. Calibration data for glucose (A) and insulin (B). (A) Concentration dependence for glucose over the 0−10 mM range in the presence of 1.28×10^{-4} g mL^{-1} Ab-E and 0.1 nM insulin. Also shown (as inset) is the portion of the electropherograms for 0 (a), 2 (b), 4 (c), 6 (d), and 8 (e) mM glucose. (B) Dependence of the free-antibody (●) and complex (○) peak currents over the concentration range over 0.01−10 nM of insulin in the presence of 1 mM glucose, 20 U mL^{-1} GDH, and 20 mM NAD^+. Also shown (as inset) are portions of electropherograms for the free-antibody peak in the presence of 0.05 (a), 0.2 (b), 1 (c), and 5 (d) nM insulin. Other conditions are the same as those in Figure 2.

hydrodynamic voltammograms of the NADH and *p*-NP products (of the enzyme and immunological reactions) indicated that a potential of +1.2 V offered the most favorable signal/background characteristics. NADH and *p*-NP displayed similar voltammetric profiles; their oxidation started at around +0.7 V and leveled off around +1.2 V. *p*-Nitrophenyl phosphate was used as a substrate for the ALP tracer due to its high stability. Increasing the applied (separation and postcolumn) potentials over the 1500−3000 V range decreased the dual-assay time from 230 to 110 s, while the baseline resolution of the NADH and *p*-NP products was maintained. Maximum mixing was observed when the separation and postcolumn voltages were similar.

Despite the huge concentration difference [millimolar (glucose) and nanomolar (insulin)] and the use of different assay principles, the new biochip responds independently to the corresponding target analytes. Figure 3A displays calibration data obtained for concentrations ranging from 0 to 10 mM glucose in the presence of insulin and anti-insulin. As is expected for biocatalytic reactions, the NADH peak increases linearly ($R^2 = 0.999$) up to a glucose concentration of 6 mM and levels off above 8 mM. The heights of both the free-antibody and the complex peaks can be used for quantitating low insulin levels. For example, Figure 3B displays the dependence of the free-antibody (●) and of the immunocomplex (○) peaks on the insulin concentration (10 pM to 10 nM range) in the presence of 1 mM glucose. While the peak of the free antibody decreases upon increasing the level of insulin, the complex peak increases with the antigen concentration; linear dynamic ranges of 0.05−2 nM ($R^2 = 0.989$) and of 0.1−1 nM ($R^2 = 0.997$) are observed for the free-antibody and complex peaks, respectively. Portions of actual electropherograms from these glucose and insulin calibration experiments are displayed in the insets. Detection limits of 10 pM and 100 μM can be estimated for insulin and glucose, respectively (based on the signal-to-noise characteristics). Overall, the data of Figure 3 indicate that both insulin and glucose can be measured reliably over their largely different clinically relevant ranges [glucose (2.5−7.2 mM) and insulin (36−179 pM)].[11,12] The linear range can be extended to accommodate higher glucose concentrations by tailoring the GDH level. The dual glucose/insulin response is highly reproducible. A series of five repetitive measurements of a mixture containing 10 pM insulin and 2 mM glucose yielded relative standard deviations of 4.7% and 4.6%, respectively, for the peak currents of the labeled-antibody and NADH peaks. The clinically relevant insulin/glucose peak ratio remained highly reproducible (with a RSD of 0.36%), reflecting the fact that both peaks are similarly influenced by experimental variables.

In summary, we have demonstrated a new biochip strategy for coupling enzymatic and immunological assays on a single-channel microfluidic device and its applicability to simultaneous glucose and insulin measurements. Such a coupling of different bioassays on the same microfluidic device reflects the versatility and integration features of such devices. The availability of a biochip capable of simultaneously monitoring both insulin and glucose holds great promise for improved management of diabetes. Crucial for the successful realization of such glucose/insulin monitoring is the integration of relevant sample pretreatment/cleanup procedures essential for whole blood analysis. The new biochip approach can be extended to the integration of other assays and additional sample handling steps, as is desired for creating versatile and miniaturized clinical analyzers. Homogeneous multiplexed immuno and/or enzyme assays can be envisioned.

Acknowledgment. Financial support from the NIH is greatly appreciated.

Supporting Information Available: Related instrumentation, procedures, and reagents (PDF). This material is available free of charge via the Internet at http://pubs.acs.org.

References

(1) Harrison, D. J.; Fluri, K.; Seiler, K.; Fan, Z. H.; Effenhauser, C. S.; Manz, A. *Science* **1993**, *261*, 895.
(2) Thorsen, T.; Maerkl, S. J.; Quake, S. R. *Science* **2002**, *298*, 580.
(3) (a) Reyes, D. R.; Iossifidis, D.; Auroux, P. A.; Manz, A. *Anal. Chem.* **2002**, *74*, 2623. (b) Auroux, P. A.; Iossifidis, D.; Reyes, D. R.; Manz, A. *Anal. Chem.* **2002**, *74*, 2637.
(4) Wang, J. *Electrophoresis* **2002**, *23*, 713.
(5) Verpoorte, E. A. *Electrophoresis* **2002**, *23*, 677.
(6) (a) Xue, Q.; Wainright, A.; Gangakhedkar, S.; Gibbons, I. *Electrophoresis* **2001**, *22*, 4000. (b) Seong, G. H.; Crooks, R. M. *J. Am. Chem. Soc.* **2002**, *124*, 13360.
(7) Schmalzing, D.; Buonocore, S.; Piggee, C. *Electrophoresis* **2000**, *21*, 3919.
(8) Colyer, C. L.; Tang, T.; Chiem, N.; Harrison, D. J. *Electrophoresis* **1997**, *18*, 1733.
(9) (a) Chiem, N.; Harrison, J. D. *Anal. Chem.* **1997**, *69*, 373. (b) Wang, J.; Ibáñez, A.; Chatrathi, M.; Escarpa, A. *Anal. Chem.* **2001**, *73*, 5323. (c) Schmalzing, D.; Koutny, L. B.; Taylor, T. A.; Nashabeh, W.; Fuchs, M. *J. Chromatogr., B* **1997**, *697*, 175.
(10) Bennington, J. L. *Saunders Dictionary & Encyclopedia of Medicine and Technology*; W. B. Saunders Co.: Philadelphia, PA, 1984.
(11) Henry, J. B. *Clinical & Diagnosis Management by Laboratory Methods*, 18th ed.; W. B. Saunders Co.: Philadelphia, PA, 1991; Chapter 1.
(12) Pagana, K. D.; Pagana, T. J. *Mosby's Diagnostic and Laboratory Test Reference*; Mosby Year Book: Missouri, 1992.

JA036067E